Immunity, Vol. 11, 191–200, August, 1999, Copyright ©1999 by Cell Press

Modulation of B Lymphocyte Antigen Receptor Signal Transduction by a CD19/CD22 Regulatory Loop

Manabu Fujimoto, Alice P. Bradney, Jonathan C. Poe, Douglas A. Steeber, and Thomas F. Tedder*
Department of Immunology
Duke University Medical Center
Durham, North Carolina 27710

Summary

CD19 and CD22 are B lymphocyte cell-surface molecules that positively and negatively regulate antigen receptor signal transduction, respectively. Biochemical studies with B cells from CD19-deficient and CD22-deficient mice indicated that these two regulatory molecules influenced each other's functions: CD22 expression negatively regulated CD19 tyrosine phosphorylation, while optimal CD22 function was dependent on CD19 expression. Functional CD19 and CD22 interactions were also assessed in vivo by generating CD19/CD22 double-deficient mice. Remarkably, the CD19 mutation was dominant to the CD22 mutation in most instances. B lymphocytes from CD19/CD22-deficient and CD19-deficient mice were functionally equivalent despite the negative influence normally provided by CD22 expression. These data collectively suggest that CD19 activates the CD22/SHP1 inhibitory pathway that then acts primarily on CD19.

Introduction

B lymphocyte responses to transmembrane stimuli regulate development, negative selection in bone marrow, activation, proliferation, and the generation of humoral responses in the periphery. The outcome of these responses is determined in part by signal transduction through the B cell antigen receptor (BCR) complex. However, a context for BCR signal transduction is provided by multiple intracellular signaling molecules and cell surface receptors that function as "response regulators" (Healy and Goodnow, 1998; Tedder, 1998). Two of the major response regulators on the surface of B cells are CD19, which forms a complex with the CD21 complement receptor (Carroll, 1998; Fujimoto et al., 1998), and CD22, a cell surface adhesion molecule (Tedder et al., 1997b). CD19 and CD22 may each associate directly with cell-surface IgM (Leprince et al., 1993; Peaker and Neuberger, 1993; Carter et al., 1997).

CD19 is a 95,000 M_r glycoprotein expressed by early pre-B cells from the time of immunoglobulin (Ig) heavy-chain gene rearrangement until plasma cell differentiation. CD19 is a member of the Ig superfamily with an ~240 amino acid cytoplasmic region containing nine tyrosine residues (Tedder and Isaacs, 1989), some of which are rapidly phosphorylated following BCR and/or CD19 ligation. CD19 regulates BCR signaling by amplifying Src-family protein tyrosine kinase (PTK) activation and mediating interactions between these PTKs and downstream effector molecules, including phosphatidylinositol-3 (PI-3) kinase and Vav (Chalupny et al., 1993; Tuveson et al., 1993; Uckun et al., 1993; Weng et al., 1994; Li et al., 1997; Sato et al., 1997a; O'Rourke et al., 1998; Fujimoto et al., 1999). In the absence of CD19 expression, B cells from gene-targeted mice are hyporesponsive to transmembrane signals and generate modest immune responses (Engel et al., 1995; Rickert et al., 1995). Uniquely, small increases in CD19 expression levels (20%–300%) in transgenic mice dramatically enhance B cell responses to transmembrane signals and predispose these mice to autoimmunity (Zhou et al., 1994; Sato et al., 1995, 1996b, 1997b). These observations suggest that CD19 expression and function are tightly regulated under normal circumstances.

CD22 is a 140,000 M_r member of the Ig superfamily expressed in the cytoplasm of pro-B and pre-B cells and on the cell surface as B cells mature to become IgD-positive (reviewed in Tedder et al., 1997b). CD22 is an adhesion receptor for sialic acid–bearing ligands expressed in serum, and on disparate hematopoietic and nonhematopoietic cells (Engel et al., 1993; Kelm et al., 1994). In addition to its potential role as a mediator of intercellular interactions, the ~140 amino acid cytoplasmic domain of CD22 contains six tyrosines that are targets for rapid phosphorylation following surface Ig or CD22 ligation (Wilson et al., 1991; Schulte et al., 1992). Negative regulatory roles for CD22 in BCR signaling are proposed to be critical for normal B cell activation (Cyster and Goodnow, 1997; Sato et al., 1998; Smith et al., 1998), since immunoreceptor tyrosine-based inhibition motifs within CD22 recruit SHP1, a potent intracellular phosphatase with inhibitory functions (Doody et al., 1995; Lankester et al., 1995; Law et al., 1996). Consistent with a negative role for CD22, B cells from CD22-deficient ($CD22^{-/-}$) mice display augmented intracellular Ca^{2+} ($[Ca^{2+}]_i$) responses after BCR ligation and exhibit characteristics of chronic stimulation (O'Keefe et al., 1996; Otipoby et al., 1996; Sato et al., 1996a; Nitschke et al., 1997). By contrast, CD22 also associates with "positive" effector molecules (Law et al., 1996; Tuscano et al., 1996). This may explain why $CD22^{-/-}$ mice generate reduced proliferative responses to BCR cross-linking (Otipoby et al., 1996; Sato et al., 1996a). Nonetheless, CD22 is a significant regulator of BCR signal transduction.

The studies cited above suggest that CD19 and CD22 reciprocally regulate BCR function. In addition, CD19 and CD22 have counterregulatory effects on mitogen-activated protein kinase activation (Tooze et al., 1997). In addition, Vav tyrosine phosphorylation is modest and transient after BCR cross-linking in $CD19^{-/-}$ B cells, yet uniquely augmented after BCR or CD19 ligation in $CD22^{-/-}$ B cells (Sato et al., 1997a). Alternatively however, CD19 and CD22 may reciprocally regulate each other's functions and thereby regulate BCR signal transduction indirectly. In support of this hypothesis, CD19

*To whom correspondence should be addressed (e-mail: thomas.tedder@duke.edu).

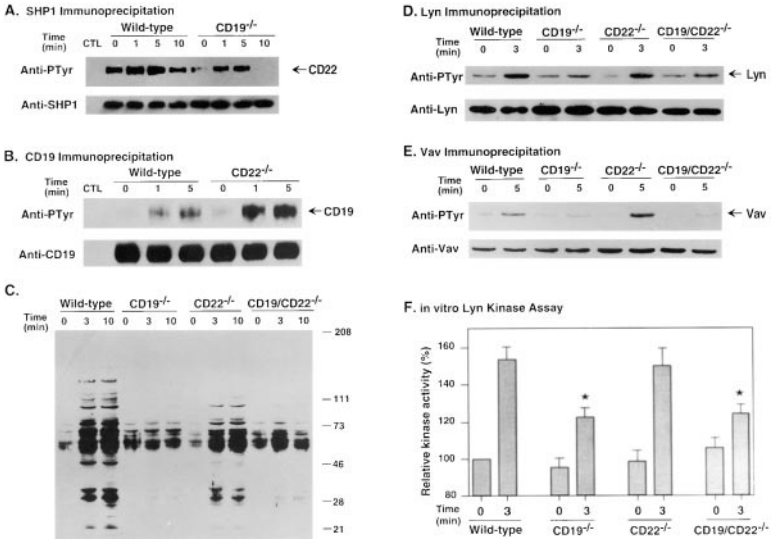

Figure 1. Regulatory Interactions between CD19 and CD22 following BCR Ligation

(A) Decreased SHP1 association with phosphorylated CD22 in CD19$^{-/-}$ B cells. Purified splenic B cells (10^7/lane) from CD19$^{-/-}$ and wild-type mice were incubated with F(ab')$_2$ anti-IgM Abs for the times shown, detergent lysed, and incubated with protein-G beads and either anti-SHP1 Ab or control rabbit IgG (CTL). Immunoprecipitated proteins were subjected to SDS-PAGE and transferred onto membranes for anti-phosphotyrosine (anti-PTyr) immunoblotting. (B) CD19 tyrosine phosphorylation in CD22$^{-/-}$ B cells. Purified wild-type or CD22$^{-/-}$ splenic B cells (4×10^7/lane) were incubated with anti-IgM before detergent lysis. Cell lysates were incubated with beads bearing either anti-CD19 or isotype-matched control (CTL) mAb. Immunoprecipitated proteins were analyzed by anti-PTyr immunoblotting. (C) Protein tyrosine phosphorylation in B cells from wild-type, CD19$^{-/-}$, CD22$^{-/-}$, and CD19/CD22$^{-/-}$ mice following BCR cross-linking. Purified splenic B cells (4×10^5/lane) incubated with either medium alone (time 0) or with anti-IgM for the indicated times were solubilized and subjected to SDS-PAGE and subsequent anti-PTyr immunoblotting. Molecular weight standards ($\times 10^{-3}$) are shown on the right. (D) Lyn and (E) Vav tyrosine phosphorylation following BCR ligation in wild-type, CD19$^{-/-}$, CD22$^{-/-}$, and CD19/CD22$^{-/-}$ B cells. Lyn and Vav were immunoprecipitated from cell lysates (10^7 cells/lane) and immunoblotted with anti-PTyr Ab (top panels). All blots were subsequently stripped and reprobed with the specific Abs to verify loading equivalency (bottom panels). In (A–E), results are representative of those obtained with at least three sets of mice. (F) Lyn kinase activity following BCR ligation. Splenic B cells (10^7) were solubilized before or after incubation with anti-IgM for 3 min, followed by immunoprecipitation with anti-Lyn Ab or control rabbit IgG. Immunoprecipitates were then incubated with cdc2(6-20)NH_2 peptide and [γ-^{32}P] ATP. The radioactivity incorporated into cdc2 peptide was quantified by scintillation counting. Relative mean ($\pm$ SEM) kinase activities are obtained from three experiments. Kinase activity is shown as percentage of wild-type B cells at 0 min, in which background and unstimulated wild-type B cells were defined as 0% and 100%, respectively. Asterisks indicate sample means significantly different from wild-type mice; $p < 0.05$.

expression is required for CD22 phosphorylation after BCR ligation (Sato et al., 1997a). In the current biochemical studies, CD19 and CD22 were found to reciprocally modulate each other's functions. Moreover, the suppressive influence of CD22 on B cell activation in vivo required CD19 expression. This suggests that, while CD19 is necessary to initiate negative regulation provided by CD22 expression, CD19 is also likely to be a major target of the CD22 inhibitory pathway.

Results

CD19 Expression Regulates SHP1 Binding to CD22

Since CD19 expression is required for optimal CD22 phosphorylation after BCR ligation (Sato et al., 1997a), and phosphorylated CD22 binds SHP1 to mediate the negative regulatory effects of CD22, regulatory interactions between CD19, CD22, and SHP1 were assessed further. SHP1 was immunoprecipitated from lysates of B cells from CD19$^{-/-}$ and wild-type mice before and after BCR cross-linking. Immunoprecipitates were subjected to sodium dodecyl sulfate-polyacrylamide gel electrophoresis (SDS-PAGE) and then electrophoretic transfer to nitrocellulose membranes. Anti-phosphotyrosine immunoblotting revealed the presence of a major tyrosine phosphorylated protein that migrated at ~140 kDa (Figure 1A). This protein was considered to be CD22 since preclearance of the cell lysates with anti-CD22 Ab depleted this band (data not shown). Similarly, this 140 kDa phosphoprotein band does not coprecipitate with SHP1 in CD22$^{-/-}$ B cells (Sato et al., 1997a). Tyrosine phosphorylated CD22 was constitutively associated with SHP1 in resting B cells (Figure 1A), and this association increased after IgM ligation in wild-type and CD19$^{-/-}$ B cells. However, relatively little phosphoCD22 coprecipitated with SHP1 from resting and activated CD19$^{-/-}$ B cells when compared with wild-type B cells (Figure 1A). SHP1 phosphorylation was similar between wild-type and CD19$^{-/-}$ B cells (data not shown). Thus, CD19 expression regulates SHP1 associations with CD22 before and after BCR ligation.

CD22 Expression Regulates CD19 Tyrosine Phosphorylation

The effect of CD22 expression on CD19 tyrosine phosphorylation was assessed by immunoprecipitating CD19 from CD22$^{-/-}$ and wild-type B cells before and after BCR cross-linking. CD19 tyrosine phosphorylation was constitutively higher in CD22$^{-/-}$ B cells and was increased significantly after BCR ligation relative to wild-type B cells (Figure 1B). Augmented CD19 tyrosine phosphorylation in CD22$^{-/-}$ B cells contrasts markedly with BCR phosphorylation, which is reduced in CD22$^{-/-}$ B cells following BCR ligation (Sato et al., 1997a).

We attempted to assess directly whether enhanced CD19 phosphorylation in CD22$^{-/-}$ B cells resulted from decreased SHP1 associations with CD22 using moth-eaten-viable (*Me^v*) mice. The *Me^v* mutation results in functionally defective SHP1 protein (Kozlowski et al., 1993). Heterozygous *me^v* (*me$^{v/+}$*) mice were used for these studies since the majority of their splenic B cells

are conventional B cells, while splenocytes of homozygous me^v (me^v/me^v) mice are almost exclusively B1 ($CD5^+$) B cells. However, the results neither supported nor contradicted the involvement of SHP1 in CD19 dephosphorylation. CD19 tyrosine phosphorylation tended to be lower in B cells from $me^{v/+}$ mice compared with their wild-type littermates following BCR ligation (four of six experiments; data not shown). By contrast, CD19 or BCR ligation induced normal $[Ca^{2+}]_i$ responses in $me^{v/+}$ B cells (data not shown). This contrasts with augmented $[Ca^{2+}]_i$ responses by $CD22^{-/-}$ B cells after BCR ligation (O'Keefe et al., 1996; Otipoby et al., 1996; Sato et al., 1996a; Nitschke et al., 1997). In me^v/me^v B cells, CD19 was not tyrosine phosphorylated at detectable levels before or following BCR ligation (data not shown). Furthermore, CD19 cross-linking failed to induce a measurable $[Ca^{2+}]_i$ increase in me^v/me^v B cells. Analogously, BCR ligation induces a reduced and blunted $[Ca^{2+}]_i$ response in B1 cells (Krop et al., 1996). Thus, although increased CD19 phosphorylation in $CD22^{-/-}$ B cells suggests that CD19 is a target of the CD22/SHP1 complex, this remains to be formally proven given the complex phenotypes of me^v mice.

Tyrosine Phosphorylation in CD19/CD22$^{-/-}$ B Cells

To further dissect the relationships between CD19 and CD22 regulation of B cell function, $CD19/CD22^{-/-}$ mice were generated. The consequences of CD19 and CD22 loss on signal transduction were evaluated by assessing total cellular protein tyrosine phosphorylation in purified B cells. Although some variation was observed between B cells from individual mice in individual experiments, overall levels of tyrosine phosphorylation in resting splenic B cells were similar among all four mouse genotypes: wild-type, $CD19^{-/-}$, $CD22^{-/-}$, and $CD19/CD22^{-/-}$. Resting B cells from $CD19^{-/-}$ mice had generally lower levels of endogenous protein tyrosine phosphorylation than resting B cells from wild-type mice in three of four experiments, while protein phosphorylation in resting B cells from $CD19/CD22^{-/-}$ mice was always slightly higher than in wild-type B cells. Nonetheless, protein phosphorylation in B cells from $CD19/CD22^{-/-}$ and $CD19^{-/-}$ mice increased modestly, if at all, after BCR ligation (Figure 1C). By contrast, protein phosphorylation increased in wild-type and $CD22^{-/-}$ B cells. Thus, BCR-induced tyrosine phosphorylation was severely impaired in $CD19/CD22^{-/-}$ and $CD19^{-/-}$ B cells, regardless of CD22 expression.

Lyn and Vav Tyrosine Phosphorylation in CD19/CD22$^{-/-}$ B Cells

The mechanism by which CD19 regulates CD22 phosphorylation was further assessed by identifying the signaling molecules affected by CD19 or CD22 loss. Since impaired activation of Src-family PTKs is a hallmark of B cells from $CD19^{-/-}$ mice (Fujimoto et al., 1999), Lyn kinase activation was assessed. Lyn tyrosine phosphorylation was only modestly increased in $CD19^{-/-}$ and $CD19/CD22^{-/-}$ B cells after BCR ligation (Figure 1D). Consistent with modest increases in phosphorylation, Lyn kinase activity in $CD19^{-/-}$ and $CD19/CD22^{-/-}$ B cells was significantly lower than that in wild-type B cells after BCR ligation (Figure 1F). This suggests that CD19 amplification of Lyn kinase activity (Fujimoto et al., 1999) is critical for optimal CD22 phosphorylation. CD19 and CD22 expression also reciprocally regulate Vav phosphorylation (Sato et al., 1997a). In this study, Vav tyrosine phosphorylation was decreased in both $CD19^{-/-}$ and $CD19/CD22^{-/-}$ B cells following BCR ligation, while Vav phosphorylation was increased in $CD22^{-/-}$ B cells (Figure 1E). Therefore, CD22 expression may negatively regulate either CD19 function or the Vav docking sites on phosphorylated CD19, or CD22 may regulate Vav phosphorylation directly.

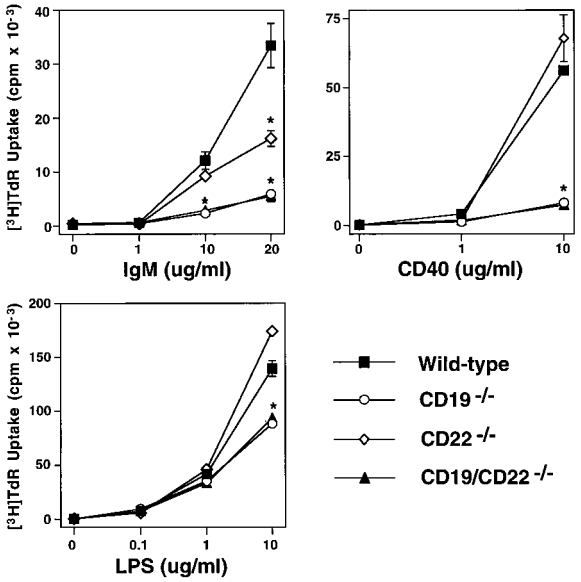

Figure 2. Proliferation of $CD19/CD22^{-/-}$ B Cells in Response to Mitogenic Signals

Spleen B cells (2×10^5/well) from wild-type, $CD19^{-/-}$, $CD22^{-/-}$, and $CD19/CD22^{-/-}$ mice were purified with anti-Thy1.2 Ab-coated magnetic beads. B cells were cultured with the indicated concentrations of anti-IgM Abs, LPS, or anti-CD40 mAb. Proliferation was assessed by the incorporation of labeled thymidine (1 μCi/well) added during the last 16 hr of 72 hr cultures. Values represent the mean values (± SEM) obtained from triplicate cultures. Mean values significantly different from wild-type proliferation levels are indicated, *$p < 0.05$. Results represent those obtained in four independent experiments.

Impaired B Cell Proliferation in CD19/CD22$^{-/-}$ Mice

The effects of CD19 and CD22 loss on B cell responses to anti-IgM, lipopolysaccharide (LPS), and CD40 ligation were assessed. In each case, proliferative responses by $CD19^{-/-}$ and $CD19/CD22^{-/-}$ B cells were remarkably similar (Figure 2). Proliferation of $CD19/CD22^{-/-}$ and $CD19^{-/-}$ B cells was reduced in response to surface IgM cross-linking (67 ± 5% and 61 ± 13% inhibition at 20 μg/ml, respectively; $p < 0.01$ in four experiments relative to wild-type B cells), LPS (30 ± 10%; 32 ± 3% at 10 μg/ml, $p < 0.05$), and anti-CD40 Ab (75 ± 5%; 71 ± 9% at 10 μg/ml, $p < 0.001$). By contrast, proliferation of $CD22^{-/-}$ B cells was augmented or normal in response to LPS or CD40 ligation as previously reported (Sato et al., 1996a). Although $CD22^{-/-}$ B cell proliferation in response to IgM ligation was reduced (55 ± 8% inhibition at 20 μg/ml, $p < 0.01$ in four experiments), the

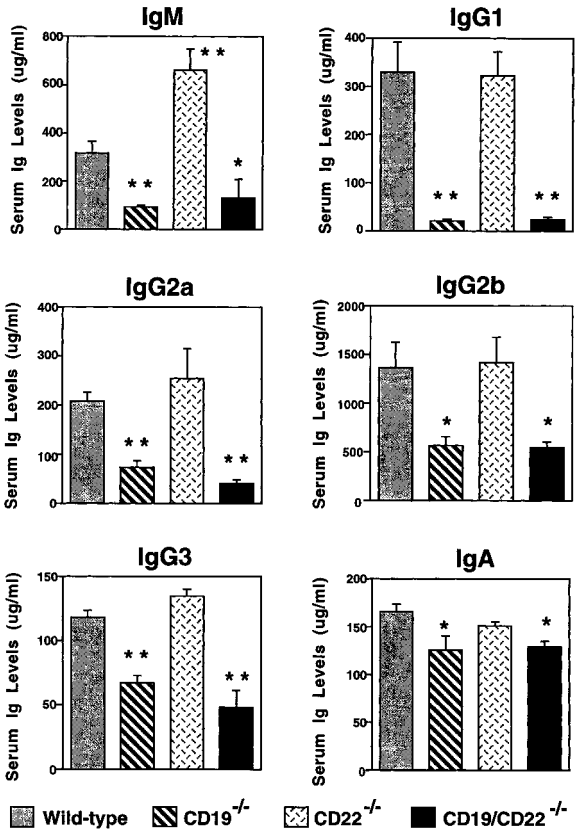

Figure 3. Serum Ig Levels

Values represent mean (± SEM) Ig levels for 5–10 wild-type (gray histograms), CD19$^{-/-}$ (striped), CD22$^{-/-}$ (speckled), and CD19/CD22$^{-/-}$ (filled) mice as determined by isotype-specific ELISA. Mean values significantly different from wild-type levels are indicated; *$p < 0.05$, ** $p < 0.01$.

combined loss of CD19 and CD22 did not cause an additive decrease in proliferation beyond the effect of CD19 loss alone (Figure 2).

Humoral Immunity in CD19/CD22$^{-/-}$ Mice

The effects of combined CD19 and CD22 loss on serum Ig levels were assessed to determine the effect on B cell differentiation. Serum levels of most Ig isotypes were reduced significantly in both CD19/CD22$^{-/-}$ and CD19$^{-/-}$ mice when compared with wild-type mice (Figure 3). On average, IgM levels in CD19/CD22$^{-/-}$ mice were reduced by 60%, IgG_1 by 93%, IgG_{2a} by 81%, IgG_{2b} by 60%, and IgG_3 by 60%. These were comparable to the decreases observed in CD19$^{-/-}$ mice: IgM reduced by 69%, IgG_1 by 94%, IgG_{2a} by 65%, IgG_{2b} by 60%, and IgG_3 by 41%. By contrast, CD22$^{-/-}$ mice had elevated serum IgM levels (209% of wild-type levels, $p < 0.005$) but normal levels of all IgG isotypes (Figure 3). Thus, the loss of CD22 did not significantly increase endogenous IgM levels in CD19$^{-/-}$ mice.

The influence of CD19 and CD22 loss on humoral immune responses was assessed by immunizing mice with the T cell-dependent antigen, 2,4-dinitrophenyl-keyhole limpet hemocyanin (DNP-KLH). Following immunization, primary and secondary IgM and IgG_1 responses in CD19/CD22$^{-/-}$ and CD19$^{-/-}$ mice were

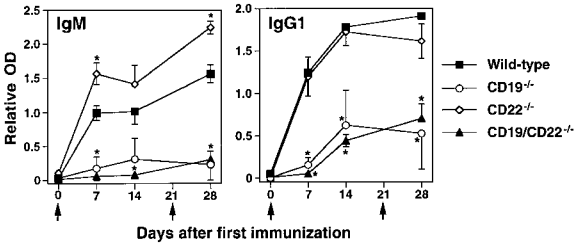

Figure 4. Humoral Immune Responses of CD19/CD22$^{-/-}$ Mice

Wild-type, CD19$^{-/-}$, CD22$^{-/-}$, and CD19/CD22$^{-/-}$ mice were injected intraperitoneally with 100 μg of DNP-KLH in complete Freund's adjuvant on days 0 and 21 (arrows) and bled at the indicated times. Serum levels of anti-DNP Abs for three to six mice of each genotype were determined by isotype-specific ELISA.

significantly lower than in wild-type mice (Figure 4). CD22$^{-/-}$ mice generated higher IgM responses than wild-type mice but similar IgG_1 responses (Figure 4). Similar results were obtained when the dilution of sera giving half-maximal OD values (t-$max_{1/2}$) in DNP-specific ELISAs was determined by linear regression analysis. Specifically, CD19/22$^{-/-}$ mice mounted primary IgM and IgG_1 responses that were only 26% and 6% of wild-type responses (t-$max_{1/2}$, 143 versus 542 for IgM; 212 versus 3,475 for IgG_1) on day 7. IgM and IgG_1 responses by CD19$^{-/-}$ mice were 54% (294) and 10% (335) of wild-type levels, while CD22$^{-/-}$ mice had increased IgM (1,354) and wild-type IgG_1 (3,076) responses. Secondary IgM and IgG_1 responses by CD19/22$^{-/-}$ and CD19$^{-/-}$ mice on day 28 were reduced >95% compared to wild-type responses (IgM; wild-type 10,615, CD19$^{-/-}$ 440, CD19/CD22$^{-/-}$ 400) (IgG_1; wild-type 113,806, CD19$^{-/-}$ 565, CD19/CD22$^{-/-}$ 942). CD22$^{-/-}$ mice had increased IgM (13,286) and wild-type IgG_1 (87,589) responses. Germinal centers were nearly absent in the spleens of CD19/CD22$^{-/-}$ mice after secondary challenge as occurs in CD19$^{-/-}$ mice (Rickert et al., 1995; Sato et al., 1995). Thus, CD19 function dominates the role of CD22 during humoral immune responses.

Decreased Peripheral B Cells in CD19/CD22$^{-/-}$ Mice

Deletion of CD19 and/or CD22 from the cell surface had only modest, if any, effects on the generation of IgM$^-$B220^{lo} pro/pre-B cells, IgM$^+$B220^{lo} immature B cells, or IgM$^+$B220^{hi} mature B cells (Figure 5A; Table 1). CD19/CD22$^{-/-}$ and CD22$^{-/-}$ mice had reduced numbers of blood B cells, while circulating B cell numbers were fairly normal in CD19$^{-/-}$ mice (Figure 5B; Table 1). Similar to blood, CD19/CD22$^{-/-}$ mice had reduced numbers of peripheral lymph node B cells. Both CD19/CD22$^{-/-}$ and CD19$^{-/-}$ mice had significantly reduced numbers of spleen B cells (40% and 44% reduction, respectively [Figure 5C; Table 1]). In most cases, reductions observed in CD22$^{-/-}$ mice were also evident in CD19/CD22$^{-/-}$ mice, and the loss of CD19 and CD22 had synergistic effects on peripheral B cell numbers.

In contrast to what was observed for most peripheral B cells, there was a significant reduction in the frequency of B220$^+$IgM$^+$ B cells in the peritoneal cavity of CD19/CD22$^{-/-}$ and CD19$^{-/-}$ mice (Figure 5D; Table 1). This

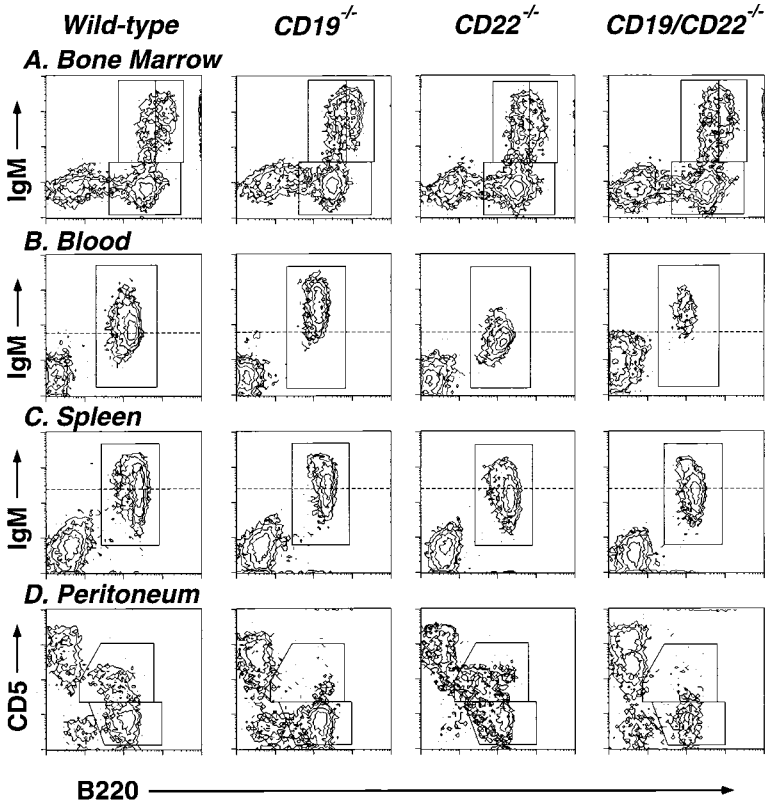

Figure 5. Lymphocytes Present in Lymphoid Tissues of CD19/CD22$^{-/-}$ Mice

Single cell suspensions of leukocytes were isolated from wild-type, CD19$^{-/-}$, CD22$^{-/-}$, and CD19/CD22$^{-/-}$ mice and examined by two-color immunofluorescence staining with flow cytometry analysis. Quadrant gates indicate negative and positive populations of cells as determined using isotype-matched unreactive control mAbs. Horizontal dashed lines in some histograms are provided for reference. The gated cell populations correspond to the cells described in Table 1 and are shown for reference. These results are representative of those obtained with 6 or 7 two-month-old mice of each genotype.

primarily resulted from severely reduced numbers of CD5^{+}B220^{lo} B1 cells in these mice. This contrasted with increased numbers of B1 cells in the peritoneum of CD22$^{-/-}$ mice. Therefore, CD19 expression is required for the generation and maintenance of B1 cells, which was not compensated for by the simultaneous loss of CD22.

Surface IgM Levels on CD19/CD22$^{-/-}$ B Cells

Although B cells mature normally in CD19$^{-/-}$ and CD22$^{-/-}$ mice, altered surface IgM expression is a characteristic feature of their B cells due to altered signaling thresholds. In the bone marrow of CD19/CD22$^{-/-}$ and CD19$^{-/-}$ mice, IgM expression levels by B220^{lo}IgM^{+} immature B cells were increased, while comparable B cells in CD22$^{-/-}$ mice expressed wild-type IgM levels (Figure 5A; Table 1). IgM levels on mature B220^{hi} B cells from CD19/CD22$^{-/-}$ and CD22$^{-/-}$ mice were normal, while IgM levels on comparable B cells from CD19$^{-/-}$ mice remained elevated. In blood, the cell-surface density of IgM was also significantly elevated on B cells from CD19/CD22$^{-/-}$ mice (Figure 5B; Table 1). However, these IgM levels were intermediate between the markedly increased levels on CD19$^{-/-}$ B cells and the significantly decreased levels found on CD22$^{-/-}$ B cells. In the spleen, surface IgM levels were reduced in CD19/CD22$^{-/-}$ and CD22$^{-/-}$ mice, while B cells from CD19$^{-/-}$ mice expressed wild-type IgM levels. In all cases, differences in cell size (light scatter properties) were not detectable for CD19$^{-/-}$, CD22$^{-/-}$, or CD19/CD22$^{-/-}$ B cells when compared with comparable wild-type B cells (data not shown). Therefore, IgM expression by CD19/CD22$^{-/-}$ B cells appeared to be synergistically regulated by both CD19 and CD22 expression.

Augmented but Delayed $[Ca^{2+}]_i$ Responses in CD19/CD22$^{-/-}$ B Cells

Both CD19 and CD22 have hallmark effects on $[Ca^{2+}]_i$ release following surface IgM cross-linking. CD19$^{-/-}$ B cells generate near normal $[Ca^{2+}]_i$ responses with a delayed peak during the acute phase and a more prolonged late phase response (Sato et al., 1997b). By contrast, CD22 loss results in dramatically increased levels of $[Ca^{2+}]_i$. Like CD22$^{-/-}$ B cells, CD19/CD22$^{-/-}$ B cells generated exaggerated $[Ca^{2+}]_i$ responses, although these responses also shared the characteristic features of $[Ca^{2+}]_i$ responses in CD19$^{-/-}$ B cells (Figure 6). Similar results were obtained with optimal or suboptimal concentration of anti-IgM Abs. These results contrast markedly with all of the responses observed earlier where CD19$^{-/-}$ and CD19/CD22$^{-/-}$ B cell responses were identical following BCR ligation. This suggests that, while synergistic interactions between CD19 and CD22 influence acute $[Ca^{2+}]_i$ flux, CD19 may not be a major target of the CD22 inhibitory pathway in $[Ca^{2+}]_i$ regulation.

Discussion

The current studies suggest that CD19 and CD22 regulate a common signaling pathway following BCR ligation. This provides a new model for how these two cell-surface molecules cooperatively interact to regulate BCR signal transduction. Biochemical results from CD19$^{-/-}$ and CD22$^{-/-}$ B cells show that both CD19 and CD22 regulate tyrosine phosphorylation after BCR ligation. In the absence of CD22 expression, CD19 was tyrosine phosphorylated at much higher levels (Figure

Table 1. Frequency, Number, and IgM Expression Levels of B Lymphocytes in CD19/CD22$^{-/-}$ Mice[a]

		Percentage of B Lymphocytes				Number of B Lymphocytes ($\times 10^{-6}$)[b]				IgM Expression (Percentage of Wild Type)[c]		
Tissue	Phenotype	Wild Type	CD19$^{-/-}$	CD22$^{-/-}$	CD19/CD22$^{-/-}$	Wild Type	CD19$^{-/-}$	CD22$^{-/-}$	CD19/CD22$^{-/-}$	CD19$^{-/-}$	CD22$^{-/-}$	CD19/CD22$^{-/-}$
Bone Marrow	B220^{lo} IgM^{-}	43 ± 4	35 ± 2[f]	45 ± 5	36 ± 3							
	B220^{lo} IgM^{+}	18 ± 2	13 ± 1	19 ± 2	15 ± 2					136 ± 4[g]	105 ± 12	144 ± 7[g]
	B220^{hi} IgM^{+}	10 ± 1	15 ± 2[f]	7 ± 1	9 ± 1					152 ± 6[g]	94 ± 6	102 ± 9
Blood[d]	B220^{+} IgM^{+}	56 ± 6	39 ± 2[f]	37 ± 5	13 ± 4[g]	3.1 ± 1	2.8 ± 0.8	1.7 ± 0.2	0.7 ± 0.4[f]	411 ± 61[g]	33 ± 5[g]	297 ± 63[f]
Spleen	B220^{+} IgM^{+}	56 ± 2	33 ± 4[g]	43 ± 5	35 ± 3[f]	45 ± 8	18 ± 4[f]	33 ± 8	20 ± 4[f]	117 ± 12	70 ± 6[g]	71 ± 6[g]
Lymph Nodes[e]	B220^{+} IgM^{+}	22 ± 4	18 ± 7	17 ± 1	10 ± 1	0.7 ± 0.3	0.9 ± 0.5	0.7 ± 0.2	0.3 ± 0.1	144 ± 7[g]	70 ± 4[g]	79 ± 8
Peritoneum	B220^{+} IgM^{+}	50 ± 6	38 ± 7	51 ± 4	23 ± 5[f]	3.4 ± 0.1	1.0 ± 0.6	5.4 ± 0.8	0.7 ± 0.3[g]			
	B220^{lo} CD5^{+}	21 ± 4	4 ± 1[g]	36 ± 3[f]	5 ± 1[g]	1.3 ± 0.2	0.2 ± 0.1[f]	2.2 ± 0.2	0.3 ± 0.1[g]			
	B220^{hi} CD5^{-}	41 ± 3	42 ± 5[f]	29 ± 3[f]	23 ± 4[f]	2.7 ± 0.5	2.2 ± 0.6	2.0 ± 0.5	1.1 ± 0.3[f]			

[a] Values represent mean (± SEM) results obtained from 6 to 7 2-month-old mice of each genotype. Numbers represent the percentage of lymphocytes (based on side and forward light scatter properties) expressing the indicated cell surface markers as determined in Figure 5 using two-color immunofluorescence staining.

[b] B cell numbers were calculated based on the total number of cells harvested from the indicated tissues.

[c] Relative cell-surface receptor densities were determined by comparing the channel numbers of the mean linear fluorescence intensity between B cells from wild-type and CD19$^{-/-}$, CD22$^{-/-}$, or CD19/CD22$^{-/-}$ mice.

[d] The values indicate the number of cells/ml.

[e] The values represent results from pooled inguinal and axillary lymph node pairs.

[f] The percentage or number was significantly different than in wild-type littermates, $p < 0.05$

[g] $p < 0.01$.

Figure 6. Ca^{2+} Responses following BCR Ligation in CD19/CD22$^{-/-}$ B Cells

Splenocytes from wild-type, CD19$^{-/-}$, CD22$^{-/-}$, and CD19/CD22$^{-/-}$ mice were loaded with indo-1 and stained with FITC-labeled anti-B220 mAb. B cells were examined for relative $[Ca^{2+}]_i$ levels by flow cytometry after gating on the B220^{+} population of cells. (A) Suboptimal or (B) optimal concentrations of Abs reactive with IgM were added to the cell mixtures at the indicated times (arrows). An increase in $[Ca^{2+}]_i$ over time is shown as an increase in the ratio of indo-1 fluorescence. Values represent the ratios of fluorescence intensity of cell populations after Ab treatment relative to the fluorescence intensity of untreated cells. These results are representative of those obtained from five independent experiments.

1B). The significance of increased CD19 phosphorylation is underscored by the finding that both BCR phosphorylation and overall protein tyrosine phosphorylation are reduced in CD22$^{-/-}$ B cells (Figure 1C; Sato et al., 1997a). Reciprocally, CD22 is hypophosphorylated in the absence of CD19 expression (Sato et al., 1997a), and CD22/SHP1 complex formation was diminished (Figure 1A). CD19 expression is thereby likely to engage the CD22/SHP1 inhibitory pathway that then appears to act primarily on CD19. Therefore, CD19 and CD22 reciprocally influence the outcome of BCR engagement (Sato et al., 1997a; Tooze et al., 1997), but these two receptors may primarily modulate BCR-mediated signaling in an interdependent fashion rather than independently.

Biochemical analysis of signaling in CD19/CD22$^{-/-}$ B cells further supports the idea that CD19 and CD22 primarily modulate BCR signaling in an interdependent fashion. Mimicking CD19$^{-/-}$ B cells, overall tyrosine phosphorylation was significantly decreased in CD19/CD22$^{-/-}$ B cells after BCR ligation (Figure 1C). Furthermore, both Lyn activation and Vav phosphorylation in CD19/CD22$^{-/-}$ B cells were reduced to the same extent as was observed in CD19$^{-/-}$ B cells (Figures 1D–1F). Since Lyn is considered to be the only tyrosine kinase that can phosphorylate CD22 (Chan et al., 1998; Cornall et al., 1998; Nishizumi et al., 1998; Smith et al., 1998), decreased Lyn activation in CD19$^{-/-}$ and CD19/CD22$^{-/-}$ B cells (Figures 1D and 1F) is consistent with a model in which CD19 directly regulates CD22 phosphorylation before and after BCR ligation. Decreased CD22 phosphorylation in the absence of CD19 expression thereby reduces SHP1 recruitment to the cell surface by phosphorylated CD22 (Figure 1A), the dominant binding partner for SHP1 in B cells (Sato et al., 1997a). While it is possible that a CD22/SHP1 complex reduces CD19 phosphorylation in wild-type B cells (Figure 1B) by regulating upstream PTK activity, wild-type levels of

Lyn, Fyn, Blk, and Syk phosphorylation were found in CD22$^{-/-}$ B cells (Figure 1D; Sato et al., 1997a). Thus, CD19 may be a major target of the CD22/SHP1 inhibitory pathway. Constitutive CD19 hyperphosphorylation may explain why B cells from CD22$^{-/-}$ mice exhibit phenotypic characteristics typical of chronically stimulated cells (Sato et al., 1996b, 1997b) and why overall tyrosine phosphorylation is reduced in CD22$^{-/-}$ B cells (Figure 1C; Sato et al., 1997a). B cells that overexpress CD19 by 3-fold exhibit phenotypic characteristics similar to CD22$^{-/-}$ B cells and have similarly reduced protein tyrosine phosphorylation levels (M. F. and T. F. T., unpublished data). Thus, constitutive CD19 hyperphosphorylation may chronically activate downstream signaling pathways that result in phenotypic changes and hypophosphorylation of intracellular signaling molecules.

Functional studies with B cells from CD19/CD22$^{-/-}$ mice validate the hypothesis that CD19 expression is necessary for CD22 function following BCR ligation. Rather than CD19 and CD22 deficiencies having additive effects, CD19 deficiency was dominant. Mitogen-induced proliferation of CD19/CD22$^{-/-}$ B cells was reduced to levels identical with CD19$^{-/-}$ B cells (Figure 2). Serum Ig levels in CD19/CD22$^{-/-}$ and CD19$^{-/-}$ mice were identical, despite increased IgM levels in CD22$^{-/-}$ mice (Figure 3). Ab responses and germinal center formation in CD19/CD22$^{-/-}$ mice were identical to the modest responses seen in CD19$^{-/-}$ mice, despite elevated IgM responses in CD22$^{-/-}$ mice (Figure 4). Spleen B cell numbers in CD19/CD22$^{-/-}$ mice were reduced as in CD19$^{-/-}$ mice (Table 1). As occurs in CD19$^{-/-}$ mice, B1 cells within the peritoneum of CD19/CD22$^{-/-}$ mice were rare, despite increased B1 cell numbers in CD22$^{-/-}$ mice (Figure 5; O'Keefe et al., 1996; Sato et al., 1996a). It thus appears that CD22 expression does not influence B cell responses to BCR engagement in the absence of CD19 expression. By contrast, CD19 and CD22 appear to have overlapping influences on unactivated B cells, particularly where a role for CD19 is absent or less pronounced. For example, CD22 expression influenced circulating B cell numbers with or without CD19 expression (Table 1). While CD19 loss results in higher IgM expression by immature B cells and CD22 loss results in lower IgM expression by more mature B cells, CD19/CD22$^{-/-}$ B cells have high IgM expression early and low IgM expression later during maturation (Table 1). Thus, CD19 and CD22 are likely to have independent influences on B cells prior to BCR ligation, but following BCR ligation the majority of CD22 function requires CD19 expression.

The mechanisms through which CD19 and CD22 expression affect BCR-induced $[Ca^{2+}]_i$ mobilization are likely to be complex. $[Ca^{2+}]_i$ responses in CD19/CD22$^{-/-}$ B cells reflected the overlapping influences of CD19 and CD22 (Figure 6). Similar to CD22$^{-/-}$ B cells, augmented $[Ca^{2+}]_i$ responses are also a feature of Lyn$^{-/-}$ and SHP-defective B cells (Cyster and Goodnow, 1995; Chan et al., 1998; Cornall et al., 1998; Nishizumi et al., 1998). This suggests that the Lyn/CD22/SHP1 pathway plays a critical role in downregulating $[Ca^{2+}]_i$ responses. However, there is a delay in the initial phase of $[Ca^{2+}]_i$ responses in Lyn$^{-/-}$ B cells (Chan et al., 1998; Cornall et al., 1998), which also occurs in CD19$^{-/-}$ B cells (Sato et al., 1997b) and CD19/CD22$^{-/-}$ B cells (Figure 6). This suggests that CD19 amplification of Lyn kinase activity may expedite efficient and rapid CD79a/b and Syk phosphorylation following BCR ligation, which may influence early phase $[Ca^{2+}]_i$ responses. The generation of wild-type $[Ca^{2+}]_i$ levels after BCR ligation in CD19$^{-/-}$ B cells is likely to result from a complex combination of positive and negative factors including normal Syk activation but decreased Lyn and CD22 phosphorylation (Fujimoto et al., 1999). CD19 has also been suggested to regulate PI-3 kinase activation (Buhl et al., 1997), which may contribute to efficient $[Ca^{2+}]_i$ mobilization by generating phosphatidylinositol trisphosphate to recruit Btk to the membrane (Buhl and Cambier, 1999). Nonetheless, the need for CD19 expression to generate CD22/SHP1 complexes at wild-type levels may explain why $[Ca^{2+}]_i$ responses are often sustained at high levels in CD19$^{-/-}$ B cells (Sato et al., 1997b). These results again suggest complex and overlapping interactions between Lyn, CD19, CD22, and SHP1 following BCR engagement, although CD19 and CD22 may modulate $[Ca^{2+}]_i$ mobilization through independent mechanisms.

The reciprocal effects of CD19 and CD22 expression on the generation and/or maintenance of peritoneal B1 cells are consistent with their reciprocal regulatory functions. CD19/CD22$^{-/-}$ and CD19$^{-/-}$ mice shared an almost complete absence of peritoneal B1 cells (Figure 5D; Table 1). Reduced numbers of peritoneal B1 cells are a hallmark phenotype of CD19$^{-/-}$, *Xid*, and *Vav*$^{-/-}$ mice, while CD22$^{-/-}$, motheaten, and Lyn$^{-/-}$ mice share increased numbers of B1 cells (reviewed in Tedder et al., 1997a). Notably, mice that overexpress CD19 also have increased numbers of peritoneal B1 cells (Sato et al., 1996b). This implies that CD19 hyperphosphorylation in CD22$^{-/-}$ mice (Figure 1B) may be responsible for the increase in B1 cell numbers. Regardless, the increase in B1 cell numbers in CD22$^{-/-}$ mice required CD19 expression.

An unexpected finding was that CD22 and SHP1 were constitutively associated in wild-type B cells (Figure 1A). However, others have also reported this association in unstimulated splenocytes (Pani et al., 1997; Cornall et al., 1998; Smith et al., 1998). Constitutive SHP1 binding may be due to low-level CD22 tyrosine phosphorylation in resting primary B cells. Similarly, CD19/Lyn/Vav complexes are constitutively assembled in splenic B cells prior to BCR ligation (Fujimoto et al., 1999). It is not possible to discern whether CD22/SHP1 and CD19/Lyn/Vav complexes are present at low levels in all primary B cells or whether they are present at higher levels in only a subset of activated B cells. However, the constitutive assembly of CD22/SHP1 and CD19/Lyn/Vav complexes in the majority of B cells would explain why the large majority of B cells in CD19$^{-/-}$, CD19-overexpressing, or CD22$^{-/-}$ mice exhibit characteristic phenotypic changes (Tedder et al., 1997a, 1997b). Generally elevated or decreased surface IgM density by the majority of B cells is an example of this, as shown in Table 1 and Figure 5. If CD19 and CD22 functions were only manifest following BCR engagement, then only a subpopulation of B cells would be affected by the absence or overexpression of CD19 and CD22. These observations suggest that regulatory interactions between CD22/SHP1 and CD19/Lyn/Vav complexes are likely to be dynamic components of resting B cell homeostasis.

Although CD19 and CD22 have both positive and negative effects on multiple signal transduction pathways, the current study indicates that CD19 and CD22 benefit from close functional interactions to regulate common pathways. CD19 expression levels are tightly regulated during B cell development (Krop et al., 1996; Sato et al., 1997b), and CD19 overexpression dysregulates tolerance and results in autoantibody production (Sato et al., 1996b; Inaoki et al., 1997). CD22 deficiency may also contribute to autoimmunity (O'Keefe et al., 1999). Similarly, Lyn has both positive and negative regulatory effects on BCR signaling (DeFranco et al., 1998), and $Lyn^{-/-}$ mice are autoimmune (Hibbs et al., 1995; Nishizumi et al., 1995; Chan et al., 1997), which is partly explained by a requirement for Lyn during CD22 and FcγRII tyrosine phosphorylation (Chan et al., 1998; Nishizumi et al., 1998; Smith et al., 1998). FcγRII function may also depend on CD19 regulation (Hippen et al., 1997). SHP1-defective B cells also have increased Src-family PTK activity (Lorenz et al., 1996; Siminovitch and Neel, 1998), and these mice are autoimmune. Therefore, tight regulation of CD19 function is likely to be a critical event for normal immunity since its expression modulates the activities of Src-family PTKs, CD22, SHP1, and FcγRII. That CD19 is a major target of CD22 regulation further emphasizes the necessity to closely control the CD19 signaling pathway and amplification of Src-family kinase activity. Alterations in CD19 and/or CD22 function or expression could thereby contribute substantially to autoimmunity or other diseases with modified B cell function.

Experimental Procedures

Mice

$CD19^{-/-}$ mice and $CD22^{-/-}$ mice were generated as described (Engel et al., 1995; Sato et al., 1996a). CD19/$CD22^{-/-}$ mice were generated through breedings of homozygous single-deficient mice. Lack of cell-surface CD19 and CD22 expression was verified by two-color fluorescence cytometry. All mice used were 2–3 months of age and were housed in a specific pathogen-free barrier facility. Control age-matched wild-type mice were generated from heterozygous breedings of $CD19^{+/-} \times CD22^{+/-}$ mice. All studies and procedures were approved by the Animal Care and Use Committee of Duke University.

Antibodies and Flow Cytometry

The mAbs used in this study included anti-CD19 (MB19-1; Sato et al., 1996b), anti-CD22 (CY34.1, TIB163), biotinylated or FITC-conjugated anti-B220 (RA3-6B2), and phycoerythrin (PE)-conjugated anti-CD5 (53-7.3, PharMingen). Antisera used included $F(ab')_2$ fragments of goat anti-mouse IgM (Cappel); anti-Lyn and anti-Vav (Santa Cruz Biotechnology); anti-SHP1 (Upstate Biotechnology) and anti-CD19 (generously provided by Dr. M. Grove, Duke University); and biotinylated, FITC-conjugated, or alkaline phosphatase-conjugated goat anti-mouse IgM, IgG, and IgA isotype-specific Abs (Southern Biotechnology Associates). PE-conjugated Streptavidin (Fischer Scientific) was used to reveal biotin-coupled Ab staining.

Single-cell suspensions were isolated from spleen, bone marrow, peripheral lymph nodes, and peritoneal cavity and counted using a hemocytometer prior to two-color immunofluorescence analysis. Retroorbital venous plexus puncture was utilized to obtain blood. Leukocytes ($0.5–1 \times 10^6$) were stained at 4°C using predetermined optimal concentrations of Abs for 20 min as described (Zhou et al., 1994). Blood erythrocytes were lysed after staining using the Coulter Whole Blood Immuno-Lyse kit. Cells with the forward and side light scatter properties of mononuclear cells were analyzed on a FACScan flow cytometer (Becton Dickinson) with fluorescence intensity shown on a 4-decade log scale. Fluorescence contours are shown as 50% log density plots. Positive and negative populations of cells were determined using unreactive isotype-matched Abs (PharMingen) as controls for background staining.

Immunoprecipitation and Western Blotting

Splenic B cells were purified by removing T cells with anti-Thy1.2 Ab-coated magnetic beads (Dynal). Cells were stimulated with $F(ab')_2$ anti-mouse IgM Abs (40 μg/ml) and lysed in buffer containing 1% Nonidet P-40, 150 mM NaCl, 50 mM Tris-HCl (pH 8.0), 1 mM Na o-vanadate, 2 mM EDTA, 50 mM NaF, and protease inhibitors. The lysates were either analyzed by SDS-PAGE or subjected to immunoprecipitation. For immunoprecipitations, the cell lysates were precleared twice with rabbit IgG plus protein G-Sepharose beads (Pharmacia Biotech), followed by incubation with protein G-beads plus specific Abs, or rabbit IgG (control) for 3 hr at 4°C. CD19 was immunoprecipitated using Affigel 10 beads (Bio-Rad), bearing anti-CD19 mAb. After washing with the lysis buffer four times, immunoprecipitates were subjected to SDS-PAGE and then electrophoretic transfer to nitrocellulose membranes. Membranes were incubated with horseradish peroxidase-conjugated anti-phosphotyrosine Ab (4G10; Upstate Biotechnology; PY99; Santa Cruz Biotechnology) and developed using an enhanced chemiluminescence kit (Pierce).

In Vitro Lyn Kinase Assay

After incubation of cell lysates with anti-Lyn Abs and protein-G beads, the beads were subsequently washed four times in lysis buffer and twice in reaction buffer (50 mM Tris-HCl, pH 7.4, 10 mM $MgCl_2$, 0.1 mM Na o-vanadate, and 1 mM DTT). The beads were then incubated in 50 μl of reaction buffer containing 10 μg of cdc2(6-20)NH_2 peptide (Upstate Biotechnology) and 10 μCi of [γ-^{32}P] ATP for 2 min at 25°C. The reactions were terminated by adding 40% TCA and spotted onto p81 phosphocellulose paper. The phosphocellulose paper was washed five times with 0.75% phosphoric acid and once with acetone. Radioactivity was quantified by scintillation counting.

B Cell Proliferation

Purified spleen B cells were cultured in 0.2 ml of culture medium in 96-well flat-bottom tissue culture plates with LPS (*E. coli* serotype 0111:B4, Sigma), $F(ab')_2$ anti-mouse IgM Abs, or anti-CD40 mAb (1C10, generously provided by Dr. M. Howard, DNAX). Proliferation was assessed by the incorporation of [^{3}H]-labeled thymidine (1 μCi/well) added during the last 16 hr of culture followed by scintillation counting. All treatments were carried out in triplicate cultures.

Mouse Immunization and Isotype-Specific ELISAs

Two month-old mice were immunized i.p. with 100 μg of DNP-KLH (Calbiochem-Novabiochem) in complete Freund's adjuvant and were boosted 21 days later. Mice were bled before and after immunization. ELISA assays were carried out as described previously (Engel et al., 1995), using affinity purified mouse IgM, IgG_1, IgG_{2a}, IgG_{2b}, IgG_3, and IgA (Southern Biotechnology Associates) to generate a standard curve. The relative Ig concentration in individual samples was calculated by comparing the mean OD obtained for triplicate wells to a semi-log standard curve of titrated standard Ab using linear regression analysis. DNP-specific Ab titers of sera were measured as above except that sample sera were added to ELISA plates coated with DNP-bovine serum albumin (5 μg/ml, Calbiochem-Novabiochem). Relative levels of hapten-specific IgM and IgG_1 were determined for each group of mice using pooled serum samples. Sera were diluted at log intervals (1:10 to $1:10^6$) and assessed for relative Ig levels as above except the results were plotted as OD versus dilution (log scale). The dilutions of sera giving half maximal OD values were determined by linear regression analysis, thus arbitrary unit per ml values were generated for comparisons between sets of sera.

Measurement of $[Ca^{2+}]_i$

Spleen cells were loaded with 1 μM indo-1-AM ester (Molecular Probes) at 37°C for 30 min. The cells were stained with FITC-conjugated anti-B220 Ab for 15 min at room temperature, washed, and resuspended at 2×10^6 cells/ml. The ratio of fluorescence (525/405

nm) of $B220^+$ cells was determined using a FACStar flow cytometer (Becton Dickinson). Baseline fluorescence ratios were collected for 1 min before $F(ab')_2$ anti-mouse IgM Abs (10 or 40 μg/ml) were added. Fluorescence ratios were collected at real time for 7 min. Results were plotted as the fluorescence ratio at 20 sec intervals with the background subtracted. An increase in the fluorescence ratio indicates an increase in $[Ca^{2+}]_i$.

Statistical Analysis

All data are shown as mean values ± SEM. Comparisons between groups were made using the Student's t test.

Acknowledgments

We thank R. Burges for technical assistance, M. Howard and M. Grove for reagents, and G. Kelsoe for helpful discussions. This work was supported by National Institutes of Health grants CA-81776, CA-54464, and HL-50985.

Received April 6, 1999; revised May 26, 1999.

References

Buhl, A.M., and Cambier, J.C. (1999). Phosphorylation of CD19 Y484 and Y515, and linked activation of phosphatidylinositol 3-kinase, are required for B cell antigen receptor-mediated activation of Bruton's tyrosine kinase. J. Immunol. *162*, 4438–4446.

Buhl, A.M., Pleiman, C.M., Rickert, R.C., and Cambier, J.C. (1997). Qualitative regulation of B cell antigen receptor signaling by CD19: selective requirement for PI3-kinase activation, inositol-1,4,5-trisphosphate production and Ca^{2+} mobilization. J. Exp. Med. *186*, 1897–1910.

Carroll, M.C. (1998). CD21/CD35 in B cell activation. Semin. Immunol. *10*, 279–286.

Carter, R.H., Doody, G.M., Bolen, J.B., and Fearon, D.T. (1997). Membrane IgM-induced tyrosine phosphorylation of CD19 requires a CD19 domain that mediates association with components of the B cell antigen receptor complex. J. Immunol. *158*, 3062–3069.

Chalupny, N.J., Kanner, S.B., Schieven, G.L., Wee, S., Gilliland, L.K., Aruffo, A., and Ledbetter, J.A. (1993). Tyrosine phosphorylation of CD19 in pre-B and mature B cells. EMBO J. *12*, 2691–2696.

Chan, V.W.F., Meng, F., Soriano, P., Defranco, A.L., and Lowell, C.A. (1997). Characterization of the B lymphocyte populations in Lyn-deficient mice and the role of Lyn in signal initiation and down-regulation. Immunity *7*, 69–81.

Chan, V.W.F., Lowell, C.A., and DeFranco, A.L. (1998). Defective negative regulation of antigen receptor signaling in Lyn-deficient B lymphocytes. Curr. Biol. *8*, 545–553.

Cornall, R.J., Cyster, J.G., Hibbs, M.L., Dunn, A.R., Otipoby, K.L., Clark, E.A., and Goodnow, C.C. (1998). Polygenic autoimmune traits: Lyn, CD22, and SHP-1 are limiting elements of a biochemical pathway regulating BCR signaling and selection. Immunity *8*, 497–508.

Cyster, J.G., and Goodnow, C.C. (1995). Protein tyrosine phosphatase 1C negatively regulates antigen receptor signaling in B lymphocytes and determines thresholds for negative selection. Immunity *2*, 13–24.

Cyster, J.G., and Goodnow, C.C. (1997). Tuning antigen receptor signaling by CD22: integrating cues from antigens and the microenvironment. Immunity *6*, 509–517.

DeFranco, A.L., Chan, V.W.F., and Lowell, C.A. (1998). Positive and negative roles of the tyrosine kinase Lyn in B cell function. Semin. Immunol. *10*, 299–308.

Doody, G.M., Justement, L.B., Delibrias, C.C., Mathews, R.J., Lin, J., Thomas, M.L., and Fearon, D.T. (1995). A role in B cell activation for CD22 and the protein tyrosine phosphatase SHP. Science *269*, 242–244.

Engel, P., Nojima, Y., Rothstein, D., Zhou, L.-J., Wilson, G.L., Kehrl, J.H., and Tedder, T.F. (1993). The same epitope on CD22 of B lymphocytes mediates the adhesion of erythrocytes, T and B lymphocytes, neutrophils and monocytes. J. Immunol. *150*, 4719–4732.

Engel, P., Zhou, L.-J., Ord, D.C., Sato, S., Koller, B., and Tedder, T.F. (1995). Abnormal B lymphocyte development, activation and differentiation in mice that lack or overexpress the CD19 signal transduction molecule. Immunity *3*, 39–50.

Fujimoto, M., Poe, J.C., Inaoki, M., and Tedder, T.F. (1998). CD19 regulates B lymphocyte responses to transmembrane signals. Semin. Immunol. *10*, 267–277.

Fujimoto, M., Poe, J.C., Jansen, P.J., Sato, S., and Tedder, T.F. (1999). CD19 amplifies B lymphocyte signal transduction by regulating Src-family protein tyrosine kinase activation. J. Immunol. *162*, 7088–7094.

Healy, J.I., and Goodnow, C.C. (1998). Positive versus negative signaling by lymphocyte antigen receptors. Annu. Rev. Immunol. *16*, 645–670.

Hibbs, M.L., Tarlinton, D.M., Armes, J., Grail, D., Hodgson, G., Maglitto, R., Stacker, S.A., and Dunn, A.R. (1995). Multiple defects in the immune system of *Lyn*-deficient mice, culminating in autoimmune disease. Cell *83*, 301–311.

Hippen, K.L., Buhl, A.M., D'Ambrosio, D., Nakamura, K., Persin, C., and Cambier, J.C. (1997). FcγRIIB1 inhibition of BCR-mediated phosphoinositide hydrolysis and Ca^{2+} mobilization is integrated by CD19 dephosphorylation. Immunity *7*, 49–58.

Inaoki, M., Sato, S., Weintraub, B.C., Goodnow, C.C., and Tedder, T.F. (1997). CD19-regulated signaling thresholds control peripheral tolerance and autoantibody production in B lymphocytes. J. Exp. Med. *186*, 1923–1931.

Kelm, S., Pelz, A., Schauer, R., Filbin, M.T., Tang, S., de Bellard, M.-E., Schnaar, R.L., Mahoney, J.A., Hartnell, A., Bradfield, P., et al. (1994). Sialoadhesin, myelin-associated glycoprotein and CD22 define a new family of sialic acid-dependent adhesion molecules of the immunoglobulin superfamily. Curr. Biol. *4*, 965–972.

Kozlowski, M., Mlinaric-Rascan, I., Feng, G.S., Shen, R., Pawson, T., and Siminovitch, K.A. (1993). Expression and catalytic activity of the tyrosine phosphatase PTP1C is severely impaired in motheaten and viable motheaten mice. J. Exp. Med. *178*, 2157–2163.

Krop, I., Shaffer, A.L., Fearon, D.T., and Schlissel, M.S. (1996). The signaling activity of murine CD19 is regulated during B cell development. J. Immunol. *157*, 48–56.

Lankester, A.C., van Schijndel, G.M., and van Lier, R.A. (1995). Hematopoietic cell phosphatase is recruited to CD22 following B cell antigen receptor ligation. J. Biol. Chem. *270*, 20305–20308.

Law, C.-L., Sidorenko, S.P., Chandran, K.A., Zhao, Z., Shen, S.-H., Fischer, E.H., and Clark, E.A. (1996). CD22 associates with protein tyrosine phosphatase 1C, Syk, and phospholipase C-γ1 upon B cell activation. J. Exp. Med. *183*, 547–560.

Leprince, C., Draves, K.E., Geahlen, R.L., Ledbetter, J.A., and Clark, E.A. (1993). CD22 associates with the human surface IgM-B cell antigen receptor complex. Proc. Natl. Acad. Sci. USA *90*, 3236–3240.

Li, X., Sandoval, D., Freeberg, L., and Carter, R.H. (1997). Role of CD19 tyrosine 391 in synergistic activation of B lymphocytes by coligation of CD19 and membrane Ig. J. Immunol. *158*, 5649–5657.

Lorenz, U., Ravichandran, K.S., Burakoff, S.J., and Neel, B.G. (1996). Lack of SHPTP1 results in src-family kinase hyperactivation and thymocyte hyperresponsiveness. Proc. Natl. Acad. Sci. USA *93*, 9624–9629.

Nishizumi, H., Taniuchi, I., Yamanashi, Y., Kitamura, D., Ilic, D., Mori, S., Watanabe, T., and Yamamoto, T. (1995). Impaired proliferation of peripheral B cells and indication of autoimmune disease in lyn-deficient mice. Immunity *3*, 549–560.

Nishizumi, H., Horikawa, K., Mlinaric-Rascan, I., and Yamamoto, T. (1998). A double-edged kinase Lyn: a positive and negative regulator for antigen receptor-mediated signals. J. Exp. Med. *187*, 1343–1348.

Nitschke, L., Carsetti, R., Ocker, B., Kohler, G., and Lamers, M.C. (1997). CD22 is a negative regulator of B-cell receptor signaling. Curr. Biol. *7*, 133–143.

O'Keefe, T.L., Williams, G.T., Davies, S.L., and Neuberger, M.S. (1996). Hyperresponsive B cells in CD22-deficient mice. Science *274*, 798–801.

O'Keefe, T.L., Williams, G.T., Batista, F.D., and Neuberger, M.S. (1999). Deficiency in CD22, a B cell-specific inhibitory receptor, is

sufficient to predispose to development of high affinity autoantibodies. J. Exp. Med. *189*, 1307–1313.

O'Rourke, L.M., Tooze, R., Turner, M., Sandoval, D.M., Carter, R.H., Tybulewicz, V.L.J., and Fearon, D.T. (1998). CD19 as a membrane-anchored adaptor protein of B lymphocytes: costimulation of lipid and protein kinases by recruitment of Vav. Immunity *8*, 635–645.

Otipoby, K.L., Andersson, K.B., Draves, K.E., Klaus, S.J., Farr, A.G., Kerner, J.D., Perlmutter, R.M., Law, C.-L., and Clark, E.A. (1996). CD22 regulates thymus-independent responses and the lifespan of B cells. Nature *384*, 634–637.

Pani, G., Siminovitch, K.A., and Paige, C.J. (1997). The motheaten mutation rescues B cell signaling and development in CD45-deficient mice. J. Exp. Med. *186*, 581–588.

Peaker, C.J.G., and Neuberger, M.S. (1993). Association of CD22 with the B cell antigen receptor. Eur. J. Immunol. *23*, 1358–1363.

Rickert, R.C., Rajewsky, K., and Roes, J. (1995). Impairment of T-cell-dependent B-cell responses and B-1 cell development in CD19-deficient mice. Nature *376*, 352–355.

Sato, S., Steeber, D.A., and Tedder, T.F. (1995). The CD19 signal transduction molecule is a response regulator of B-lymphocyte differentiation. Proc. Natl. Acad. Sci. USA *92*, 11558–11562.

Sato, S., Miller, A.S., Inaoki, M., Bock, C.B., Jansen, P.J., Tang, M.L.K., and Tedder, T.F. (1996a). CD22 is both a positive and negative regulator of B lymphocyte antigen receptor signal transduction: altered signaling in CD22-deficient mice. Immunity *5*, 551–562.

Sato, S., Ono, N., Steeber, D.A., Pisetsky, D.S., and Tedder, T.F. (1996b). CD19 regulates B lymphocyte signaling thresholds critical for the development of B-1 lineage cells and autoimmunity. J. Immunol. *157*, 4371–4378.

Sato, S., Jansen, P.J., and Tedder, T.F. (1997a). CD19 and CD22 reciprocally regulate Vav tyrosine phosphorylation during B lymphocyte signaling. Proc. Natl. Acad. Sci. USA *94*, 13158–13162.

Sato, S., Steeber, D.A., Jansen, P.J., and Tedder, T.F. (1997b). CD19 expression levels regulate B lymphocyte development: human CD19 restores normal function in mice lacking endogenous CD19. J. Immunol. *158*, 4662–4669.

Sato, S., Tuscano, J.M., Inaoki, M., and Tedder, T.F. (1998). CD22 negatively and positively regulates signal transduction through the B lymphocyte antigen receptor. Semin. Immunol. *10*, 287–297.

Schulte, R.J., Campbell, M.A., Fischer, W.H., and Sefton, B.M. (1992). Tyrosine phosphorylation of CD22 during B cell activation. Science *258*, 1001–1004.

Siminovitch, K.A., and Neel, B.G. (1998). Regulation of B cell signal transduction by SH2-containing protein-tyrosine phosphatases. Semin. Immunol. *10*, 329–347.

Smith, K.G.C., Tarlinton, D.M., Doody, G.M., Hibbs, M.L., and Fearon, D.T. (1998). Inhibition of the B cell by CD22: a requirement for Lyn. J. Exp. Med. *187*, 807–811.

Tedder, T.F. (1998). Response-regulators of B lymphocyte signaling thresholds provide a context for antigen receptor signal transduction. Semin. Immunol. *10*, 259–265.

Tedder, T.F., and Isaacs, C.M. (1989). Isolation of cDNAs encoding the CD19 antigen of human and mouse B lymphocytes: a new member of the immunoglobulin superfamily. J. Immunol. *143*, 712–717.

Tedder, T.F., Inaoki, M., and Sato, S. (1997a). The CD19/21 complex regulates signal transduction thresholds governing humoral immunity and autoimmunity. Immunity *6*, 107–118.

Tedder, T.F., Tuscano, J., Sato, S., and Kehrl, J.H. (1997b). CD22, a B lymphocyte-specific adhesion molecule that regulates antigen receptor signaling. Annu. Rev. Immunol. *15*, 481–504.

Tooze, R.M., Doody, G.M., and Fearon, D.T. (1997). Counterregulation by the coreceptors CD19 and CD22 of MAP kinase activation by membrane immunoglobulin. Immunity *7*, 59–67.

Tuscano, J.M., Engel, P., Tedder, T.F., Agarwal, A., and Kehrl, J.H. (1996). Involvement of p72syk kinase, p53/56lyn kinase and phosphatidyl inositol-3 kinase in signal transduction via the human B lymphocyte antigen CD22. Eur. J. Immunol. *26*, 1246–1252.

Tuveson, D.A., Carter, R.H., Soltoff, S.P., and Fearon, D.T. (1993). CD19 of B cells as a surrogate kinase insert region to bind phosphatidylinositol 3-kinase. Science *260*, 986–989.

Uckun, F.M., Burkhardt, A.L., Jarvis, L., Jun, X., Stealey, B., Dibirdik, I., Myers, D.E., Tuel-Ahlgren, L., and Bolen, J.B. (1993). Signal transduction through the CD19 receptor during discrete developmental stages of human B-cell ontogeny. J. Biol. Chem. *268*, 21172–21184.

Weng, W.K., Jarvis, L., and LeBien, T.W. (1994). Signaling through CD19 activates vav/mitogen-activated protein kinase pathway and induces formation of a CD19/vav/phosphatidylinositol 3-kinase complex in human B cell precursors. J. Biol. Chem. *269*, 32514–32521.

Wilson, G.L., Fox, C.H., Fauci, A.S., and Kehrl, J.H. (1991). cDNA cloning of the B cell membrane protein CD22: a mediator of B-B cell interactions. J. Exp. Med. *173*, 137–146.

Zhou, L.-J., Smith, H.M., Waldschmidt, T.J., Schwarting, R., Daley, J., and Tedder, T.F. (1994). Tissue-specific expression of the human CD19 gene in transgenic mice inhibits antigen-independent B lymphocyte development. Mol. Cell. Biol. *14*, 3884–3894.